Academic Journal of Science and Technology
ISSN: 2771-3032 | Vol. 14, No. 3, 2025

Genesis of the Dolomite in the Qixia Formation at Laogongqiao Village, Huaying Mountain

Yihong Liu

School of Resources & Environment, Henan Polytechnic University, Jiaozuo, China

Abstract: The dolomite in the Qixia Formation of the Sichuan Basin holds significant exploration prospects and potential for forming high-quality reservoirs. However, due to the complex types of dolomite in the Qixia Formation, it is necessary to conduct an in-depth study on the genesis of different types of dolomite. Leopard-spotted dolomitic limestone, microcrystalline dolomite, and coexisting limestone all exhibit characteristics of light rare earth element (LREE) depletion, positive La anomaly, negative Ce anomaly, slight positive Gd anomaly, and significant enrichment of Y. Their rare earth element (REE) distribution patterns are similar to seawater, suggesting that the diagenetic fluid source is likely seawater. However, the saddle-shaped dolomite cement shows distinct positive Eu and Gd anomalies and a right-tilting REE distribution pattern, indicating a hydrothermal origin. Carbon and oxygen isotope analyses show that the carbon-oxygen ratios of leopard-spotted dolomitic limestone and coexisting limestone fall within the Early Permian seawater carbon-oxygen isotope range. Combining this with the larger intergranular pores in the spotted zones, it can be concluded that dolomitization occurred in a grain-shoal environment. In contrast, the microcrystalline dolomite exhibits negative $\delta^{13}C$ and positive $\delta^{18}O$ values, which are primarily caused by a low sea level during the early transgression, leading to the presence of air with different densities in the confined environment between crystals. The Sr values of microcrystalline dolomite also suggest a semi-saline water sedimentary environment.

Keywords: Qixia Formation; Dolomite; Diagenetic Fluid; Sedimentary Environment.

1. Introduction

Dolomite reservoirs play a crucial role in carbonate rock oil and gas exploration. Therefore, domestic and international geological experts and scholars have been engaged in long-term studies on dolomite, with a particular focus on the genesis of dolomite. In recent years, natural gas exploration of the Permian Qixia Formation dolomite reservoirs in the Sichuan Basin has become an area of significant interest. However, there is still no unified framework for the genesis of dolomite, with various models proposed, such as mixed-water dolomitization (Stahl, 1977), burial dolomitization (Liao Xiaoman et al., 2012), basalt leaching dolomitization (Jin Zhenkui et al., 1999), and hydrothermal dolomitization (Zhao Wenzhi et al., 2018). These models have been developed by geologists through continuous exploration and study in the field. Most of these findings and understandings have been approached from the perspective of the entire basin or regional scale, focusing on the exploration of dolomite genesis. However, the applicability of these models to the dolomite genesis in the Qixia Formation of a specific outcrop profile remains to be discussed. Field outcrops and drilling data indicate that dolomite reservoirs in the Qixia Formation of the Sichuan Basin, particularly the pore-type dolomite reservoirs, exhibit rapid lateral variation and strong heterogeneity, which increases the difficulty of exploration. Therefore, this paper takes the dolomite in the Qixia Formation at the Laogongqiao Village outcrop in the eastern Sichuan Basin as an example. Based on the analysis of macroscopic and microscopic features of the field outcrop, combined with the regional tectonic background, the study employs geochemical element testing and other methods to analyze the types and characteristics of the dolomite in the profile, thereby discussing the dolomitization model. The goal is to provide more theoretical evidence for dolomitization research in the Sichuan Basin and to offer valuable support for the exploration of dolomite reservoirs in the region.

2. Geological Background

Laogongqiao Village is located in the core region of the eastern Sichuan fold belt within the Sichuan Basin, at the center of the Huaying Mountain fan-shaped structural system. It lies to the east of the Huaying Mountain fault zone and to the west of the Qiyao Mountain fault zone. The geological structure of the area is complex, with significant fold development, predominantly consisting of compound anticlines. The fault zones exhibit an arcuate distribution from north to south, extending from the southern part of Tianchi in Guang'an City to the southern part of Pijia Mountain in Hechuan City.

During the Permian, the Sichuan Basin was situated near the equator in a stable tectonic setting, representing a passive continental margin environment, conducive to the proliferation of abundant biological life in a warm and humid climate (Li Jianghai et al., 2013). The Caledonian movement at the end of the Silurian led to the final formation of the Leshan–Longnüsi paleo-uplift, which had already begun to take shape during the Late Ediacaran period (Zhang Shuichang et al., 2007). This uplift continued to influence Permian sedimentation, thereby controlling the sedimentary pattern of the Qixia Formation, with high sedimentation in the southwest and low sedimentation in the northeast. At the end of the Carboniferous, seawater withdrew from the Yangtze platform. After a brief sedimentary hiatus, a large-scale marine transgression began in the Early Permian, and the entire basin widely received carbonate sediments with a simple sedimentary environment and stable thickness (Hao Yi et al., 2020). The Qixia Formation started to accumulate during this period. By the Middle Permian, extensional activities on the Yangtze Plate reached a peak, and the stable sedimentation of carbonates essentially covered the entire

South China continent, forming the largest transgressive phase of the Late Paleozoic. At the end of the Middle Permian, tectonic movements such as the uplifting, Dongwu movements, and the Emei rift movements in the Upper Yangtze region reached their climax, leading to the widespread distribution of continental basalt along the western edge of the Upper Yangtze, and the entire South China plate began to rise and undergo exposure (Zhao Zongju et al., 2011). By the Late Permian, as the North China Plate shifted northward, the Mianli Ocean opened, and extensional movements within the South China Plate intensified (Luo Zhili et al., 1988), further altering the regional geographic pattern.

At the Laogongqiao Village outcrop, the total exposed thickness of the Qixia Formation reaches 133.6 meters. Its upper part contacts the thin-bedded nodular limestone with a parallel unconformity, while the lower part exhibits a conformable contact with the siltstone of the Liangshan Formation. The lower section of the Qixia Formation consists of a medium-thick layer of light gray massive microcrystalline dolomite, approximately 6 meters thick. The lower part of this microcrystalline dolomite layer is in parallel conformable contact with the Liangshan Formation, while the upper part transitions into mud-crystal wackestone. The middle section of the Qixia Formation is mainly composed of interbedded limestone and mudstone, exhibiting certain sedimentary rhythmic characteristics, with local occurrences of siliceous nodule limestone. Near the top of the Qixia Formation, leopard-spotted dolomitic limestone is exposed, with the upper part consisting of mud-crystal wackestone and mudstone, and the lower part comprising siliceous nodule limestone and gray medium-thick-layered mudstone. Additionally, siliceous limestone contains saddle-shaped dolomite cement fillings.

3. Geochemical Characteristics

3.1. REE Characteristics of Dolomite and Coexisting Rocks

During rock formation, different diagenetic fluids contain varying trace elements and rare earth elements (REEs), leading to distinct trace element content and REE distribution patterns. These differences provide a valuable means to identify diagenetic fluid types and study diagenetic processes (Klein and Beukes, 1989). In this study, we utilized LA-ICP-MS for micro-area point analysis of various dolomite and coexisting rocks in the study profile. After data processing (where SN denotes data standardized using the PAAS standard), we selected total REE content, light-to-heavy REE ratio, the degree of positive and negative anomalies of individual elements, and the Y/Ho ratio for comprehensive analysis of the fluid source and nature of the studied rocks, to better understand the genesis of the dolomite.

The total REE content of the leopard-spotted dolomitic limestone's dolomitic portion ranges from 1.39 to 1.56 μg/g, with an average of 1.46 μg/g, which is relatively low. The light-to-heavy REE ratio ranges from 0.66 to 0.74, with an average of 0.69. The δPr value ranges from 1.06 to 1.18, with an average of 1.09, indicating a negative Ce anomaly (Bau and Dulski, 1996). The δCe value ranges from 0.76 to 0.86, with an average of 0.82, representing a positive La anomaly (Bau and Dulski, 1996). The Eu/Eu* value ranges from 0.90 to 0.96, with an average of 0.93, showing an overall negative anomaly. The Y/Ho value ranges from 38.23 to 38.66, with an average of 38.41, which is lower than the normal seawater value (44–76) but higher than the values for river or estuarine waters (25–28), suggesting slight influence from hydrothermal or atmospheric freshwater (Wang Yuhang et al., 2018). The δGd value ranges from 1.05 to 1.15, with an average of 1.09, showing a slight positive anomaly.

The total REE content of the microcrystalline dolomite ranges from 1.57 to 2.50 μg/g, with an average of 2.09 μg/g, which is still relatively low. The light-to-heavy REE ratio ranges from 0.53 to 0.78, with an average of 0.68. The δPr value ranges from 1.04 to 1.09, with an average of 1.07, indicating a negative Ce anomaly (Bau and Dulski, 1996). The δCe value ranges from 0.76 to 0.86, with an average of 0.82, representing a positive La anomaly (Bau and Dulski, 1996). The Eu/Eu* value ranges from 1.15 to 1.16, with an average of 1.16, indicating a slight positive anomaly, suggesting influence from hydrothermal fluids (Meyer et al., 2012). The Y/Ho value ranges from 35.12 to 36.37, with an average of 35.52, indicating slight influence from hydrothermal or atmospheric freshwater (Wang Yuhang et al., 2018). The δGd value ranges from 1.10 to 1.27, with an average of 1.17, showing a slight positive anomaly.

The coexisting rocks with dolomite in the study profile are primarily limestone, with an average REE content of 0.72 μg/g, which is relatively low. The light-to-heavy REE ratio has an average value of 0.52. The average δPr value is 1.12, greater than 1, indicating a negative Ce anomaly (Bau and Dulski, 1996). The average δCe value is 0.83, less than 1, indicating a positive La anomaly (Bau and Dulski, 1996). The Eu/Eu* value has an average value of 0.84, showing a negative anomaly. The average Y/Ho value is 30.82, suggesting slight influence from hydrothermal or atmospheric freshwater (Wang Yuhang et al., 2018). The average δGd value is 1.15, indicating a slight positive anomaly.

The average REE content of the saddle-shaped dolomite cement is 0.79 μg/g, which is relatively low. The light-to-heavy REE ratio averages 7.21. The average δPr value is 0.93, less than 1. The average δCe value is 0.93, less than 1, indicating a positive La anomaly (Bau and Dulski, 1996). The average Eu/Eu* value is 3.51, showing a significant positive anomaly. The average Y/Ho value is 39.03. The average δGd value is 2.66, showing a positive anomaly.

The calculation formulas for these indicators are as follows:

$\delta Pr = 2PrSN / (CeSN + NdSN)$

$\delta Ce = 2CeSN / (LaSN + PrSN)$

$\delta Gd = GdSN / (0.33SmSN + 0.67TbSN)$

$Eu/Eu^* = Eu / (0.67SmSN + 0.33TbSN)$ (Bau and Dulski, 1996).

3.2. Carbon and Oxygen Isotopic Characteristics of Dolomite and Associated Rocks

The $\delta^{18}O$ values of the fine-grained dolomite range from -2.508‰ to 0.877‰, with an average of -1.363‰, and the $\delta^{13}C$ values range from -1.272‰ to -2.603‰, with an average of 0.637‰. The $\delta^{18}O$ values of the limestone range from -7.854‰ to -3.415‰, with an average of -5.311‰, and the $\delta^{13}C$ values range from 3.044‰ to 4.695‰, with an average of 4.244‰. The $\delta^{18}O$ average of the spotted dolomitic limestone is -5.389‰, and the $\delta^{13}C$ average is 3.769‰. The $\delta^{18}O$ average of the spotted dolomitic limestone is 5.072‰, and the $\delta^{13}C$ average is 4.164‰. The carbon and oxygen isotopic data and their intersection with the Early Permian seawater range are shown in Figure 1.

From Figure 1, it is evident that the carbon and oxygen isotopic values of the spotted dolomitic limestone fall within the Early Permian seawater isotopic range, and the values of the spotted dolomitic limestone are higher than those of the spotted dolomitic parts. The limestone from the Qixia Formation predominantly falls within this range, whereas the fine-grained dolomite shows a negative $\delta^{13}C$ value and a significantly positive $\delta^{18}O$ value, indicating that its deposition environment was more restricted (Chen Rongkun, 1994).

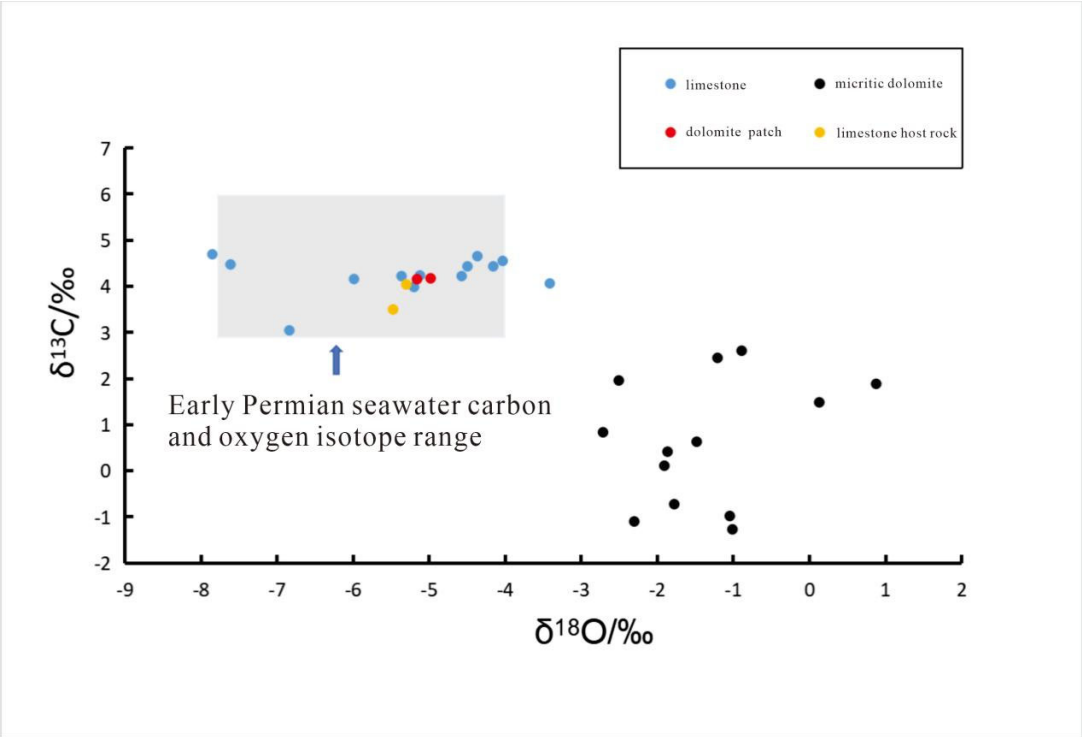

Figure 1. Carbon and Oxygen Isotopic Cross-Plot

3.3. Major Trace Element Characteristics of Dolomite and Associated Rocks

The Na content in the cloudy portion of the spotted dolomitic limestone ranges from 299.00 to 693.00 μg/g, with an average of 546.33 μg/g. The Mg content has an average of 109,733.33 μg/g, which is very high. The Sr content has an average of 2,699.33 μg/g, greater than 100 μg/g, indicating a freshwater depositional environment (Li Chengfeng et al., 1988). The Mn content averages 25.40 μg/g, which is relatively low, while the Fe content averages 2.97 μg/g, also low. The Mn/Sr ratio is low, with an average of 0.01, far less than 2, indicating that the rock retains more original seawater information (Zhong Shoukang et al., 2020). The U/Th ratio has an average value of 20.01, which is greater than 1, indicating hydrothermal alteration (Rona, 1978).

The Na content in the fine-grained dolomite averages 388.67 μg/g. The Mg content has an average of 110,033.33 μg/g, which is extremely high. The Sr content has an average of 92.63 μg/g, which falls between 60–100 μg/g, indicating a brackish water depositional environment (Li Chengfeng et al., 1988). The Mn content averages 168.10 μg/g, which is relatively low, while the Fe content averages 1,922.33 μg/g, slightly higher. The Mn/Sr ratio has an average value of 1.78, which is less than 2, indicating the rock retains more original seawater information (Zhong Shoukang et al., 2020). The U/Th ratio has an average of 12.05, indicating hydrothermal alteration (Roma, 1978).

The Na content in the limestone averages 114.80 μg/g. The Mg content has an average of 3,205.00 μg/g, which is lower than the other two rock types. The Sr content has an average of 1,316.00 μg/g, indicating a freshwater depositional environment (Li Chengfeng et al., 1988). The Mn content averages 7.52 μg/g, which is low, while the Fe content averages 17.60 μg/g, also low. The Mn/Sr ratio averages 0.006, which is far less than 2, indicating that the rock retains more original seawater information (Zhong Shoukang et al., 2020). The U/Th ratio averages 25.79, indicating hydrothermal alteration (Roma, 1978).

4. Origin of Dolomite

4.1. Fine-Grained Dolomite and Spotted Dolomitic Limestone

In terms of rare earth element (REE) composition, the fine-grained dolomite and spotted dolomitic portions show slightly lower total REE content compared to the limestone, with the heavy REE elements being more enriched. This composition is similar to that of seawater's REE structure, and all three types exhibit features such as a positive anomaly in La, a negative anomaly in Ce, a slight positive anomaly in Gd, and a significant enrichment of Y. From the REE distribution pattern (Figure 2), it is evident that the fluid sources for the associated limestone, fine-grained dolomite, and spotted dolomitic portions are all seawater-derived. Additionally, seawater-derived fluids lack Fe and Mn, which is consistent with the characteristics of all three rock types. Furthermore, the Mn/Sr ratio for all three is less than 2, indicating a greater retention of original seawater information (Zhong Shoukang et al., 2020).

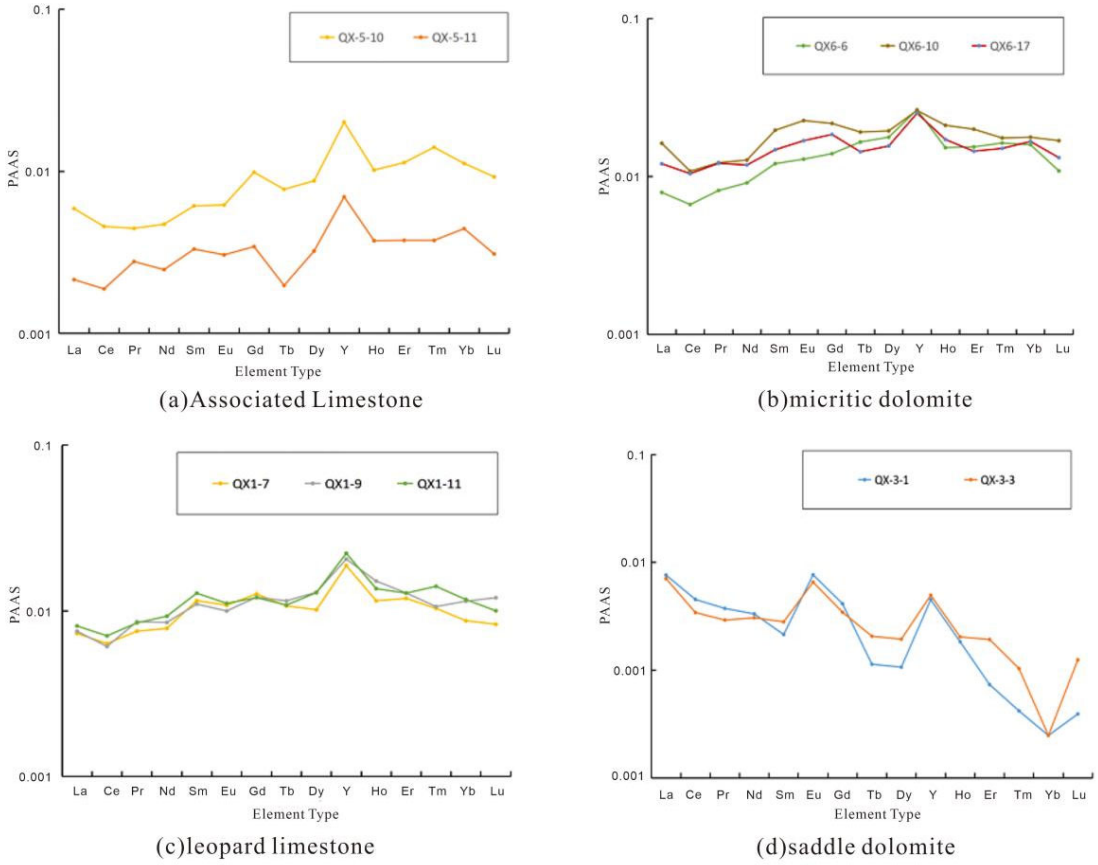

Figure 2. REE Distribution Pattern

The isotopic data from the carbon and oxygen cross-plot (Figure 1) show that the origin of the cementing fluids for the spotted dolomitic limestone and Qixia Formation limestone is seawater, while the fine-grained dolomite exhibits a negative $\delta^{13}C$ value and a positive $\delta^{18}O$ value. This suggests that its depositional environment was a restricted setting, such as tidal flats, tidal zones, or lagoons, where interstitial spaces were occupied by air and seawater. This would lead to $\delta^{13}C$ values that are low positive or close to zero, and $\delta^{18}O$ values that are relatively higher (Chen Rongkun, 1994). Research indicates that the carbon isotopic composition of marine carbonate rocks is mainly controlled by the oxidation and burial of organic carbon, and most high sea-level periods fall within the stage of rapid organic carbon burial (Huang Sijing, 1997). The fine-grained dolomite developed in the early stage of Qixia Formation deposition, in a relatively low-sea-level transgressive environment, so organic carbon burial was relatively impacted, leading to a lower $\delta^{13}C$ value. The average Sr content of 92.63 μg/g further supports this.

The positive Eu anomaly generally results from hydrothermal fluids that are chemically reducing and have temperatures above 200°C. However, this anomaly is diminished or eliminated when the seawater volume is very large (Bau et al., 2010). The fine-grained dolomite shows a weak positive Eu anomaly, suggesting that it was affected by hydrothermal alteration during diagenesis. The Y/Ho ratio for all three types is not as high as that of normal seawater (which ranges between 44–76), but it is higher than that of river or estuarine water (25–28), indicating mild influence from hydrothermal or atmospheric freshwater (Nozaki et al., 1997). Furthermore, the low U/Th ratio indicates hydrothermal alteration (Rona, 1978).

4.2. Saddle-Shaped Dolomite Cement

Previous research on the origin of the saddle-shaped dolomite cement in the Qixia Formation of the Sichuan Basin has generally agreed that it is hydrothermal in origin.

From a geochemical perspective, the saddle-shaped dolomite cement exhibits significant positive anomalies in Eu and Gd, with average values of 3.51 and 2.66, respectively, which are much higher than those of other rock types. $Ce/Ce^* < 1$ and $0.9 < Pr/Pr^* < 1$ indicate that the diagenetic environment of the saddle-shaped dolomite cement was more reducing in nature (Alibo and Nozaki, 1999). The distribution pattern (Figure 2) shows that, in addition to the obvious positive anomalies in Eu and Gd, the REE pattern is right-leaning, which contrasts with the left-leaning pattern of seawater. This suggests that the formation of the saddle-shaped dolomite cement was primarily controlled by reducing mantle hydrothermal fluids during tectonic activity.

5. Conclusion

The fine-grained dolomite in the Qixia Formation of the Huaying Mountains, at the Laogongqiao Village section, was primarily formed through percolation-reflux processes in restricted environments like tidal flats during the early diagenetic period. The cloudy part of the spotted dolomitic limestone was formed through similar processes in particle shoals during the same period, both of which were later affected by mild hydrothermal alteration during the Dongwu Movement. The saddle-shaped dolomite cement was formed by reducing hydrothermal fluids rising along faults during intense tectonic activity, followed by precipitation in voids.

References

[1] Alibo D S, Nozaki Y. Rare earth elements in seawater: particle association, shale-normalization, and Ce oxidation[J]. Geochimica et Cosmochimica Acta, 1999. 63(3): 363-372.

[2] Bau M, Balan S, Schmidt K, Koschinsky A. Rare earth elements in mussel shells of the Mytilidae family as tracers for hidden and fossil high-temperature hydrothermal systems[J]. Earth and Planetary Science Letters, 2010. 299(3): 310-316.

[3] Bau M, Dulski P. Distribution of yttrium and rare-earth elements in the Penge and Kuruman iron-formations, Transvaal Supergroup, South Africa[J]. Precambrian Research, 1996. 79(1): 37-55.

[4] Klein C, Beukes N J. Geochemistry and sedimentology of a facies transition from limestone to iron-formation deposition in the early Proterozoic Transvaal Supergroup, South Africa[J]. Economic Geology, 1989. 84(7): 1733-1774.

[5] Meyer E E, Quicksall A N, Landis J D, Link P K, Bostick B C. Trace and rare earth elemental investigation of a Sturtian cap carbonate, Pocatello, Idaho: Evidence for ocean redox conditions before and during carbonate deposition[J]. Precambrian Research, 2012. 192-195: 89-106.

[6] Nozaki Y, Zhang J, Amakawa H. The fractionation between Y and Ho in the marine environment[J]. Earth and Planetary Science Letters, 1997. 148(1): 329-340.

[7] Rona P A. Magnetic signatures of hydrothermal alteration and volcanogenic mineral deposits in oceanic crust[J]. Journal of Volcanology and Geothermal Research, 1978. 3(1): 219-225.

[8] Stahl W J. Carbon and nitrogen isotopes in hydrocarbon research and exploration[J]. Chemical Geology, 1977. 20: 121-149.

[9] Chen Rongkun. Application of Stable Oxygen and Carbon Isotopes in the Diagenetic Environment of Carbonate Rocks. Journal of Sedimentology, 1994(04): 11-21.

[10] Hao Yi, Gu Mingfeng, Wei Dongxiao, Pan Liyin, Lü Yuzhen. Sedimentary Characteristics and Reservoir Distribution Patterns of the Permian Qixia Formation in the Sichuan Basin. Marine Petroleum Geology, 2020, 25(03): 193-201.

[11] Huang Sijing. Carbon and Strontium Isotope Study of Late Paleozoic Marine Carbonate Rocks in the Upper Yangtze Platform Area. Acta Geologica Sinica, 1997(01): 45-53.

[12] Jin Zhenkui, Feng Zengzhao. Formation Mechanism of the Lower Permian Dolomite in Eastern Yunnan—Western Sichuan: Basalt Leaching Dolomitization. Journal of Sedimentology, 1999(03): 383-389.

[13] Li Chengfeng, Xiao Jifeng. Trace Element Study of Paleo-Salinity in the Shahejie Formation of the Dongying Basin, Shengli Oilfield. Journal of Sedimentology, 1988(04): 100-107.

[14] Li Jianghai, Li Weibo, Wang Honghao, Zhang Huatian, Mao Xiang. Kinematic Analysis of Plate Collision during the Late Paleozoic Pangaea Aggregation. Geological Review, 2013, 59(06): 1047-1059.

[15] Liao Xiaoman, Zhang Benjian, Xu Houwai, Zhang Fan, Qin Xueyuan. Diagenesis of the Middle Permian Reservoir in Western Sichuan Region. Xinjiang Petroleum Geology, 2012, 33(03): 312-315.

[16] Luo Zhili, Jin Yizhong, Zhu Kuiyu, Zhao Xikui. On the Emei Rift Movement of the Upper Yangtze Platform. Geological Review, 1988(01): 11-24.

[17] Wang Yuhang, Zhu Yuanyuan, Huang Jiandong, Song Huyue, Du Yong, Li Zhe. Application of Rare Earth Elements in Marine Carbonate Rocks for Paleoenvironmental Studies. Earth Science Progress, 2018, 33(09): 922-932.

[18] Zhang Shuichang, Liang Digang, Zhu Guangyou, Zhang Xingyang, Zhang Baomin, Chen Jianping, Zhang Bin. Geological Basis for the Formation of China's Marine Oil and Gas Fields. Science Bulletin, 2007, 52(A01): 13.

[19] Zhao Wenzhi, Shen Anjiang, Qiao Zhanfeng, Pan Liyin, Hu Anping, Zhang Jie. Genetic Types, Identification Features, and Reservoir Space Genesis of Dolomite. Petroleum Exploration and Development, 2018, 45(06): 923-935.

[20] Zhao Zongju, Luo Jiahong, Zhang Yunbo, Wu Xingning, Pan Wenqing. Cambrian Sequence Stratigraphy and Paleogeography of the Tarim Basin. Acta Petroleum Sinica, 2011, 32(06): 937-948.

[21] Zhong Shoukang, Li Ling, Tan Xiucheng, Sun Jian, Wang Lichao, Huang Daojun, Hou Yundong, Dong Shaofeng, Bao Hongping. Formation and Diagenetic Evolution of Medium-to-Coarse Crystalline Dolomite in the Ma5 Member of the Middle Eastern Ordos Basin. Journal of Chengdu University of Technology (Natural Science Edition), 2020, 47(06): 691-710.